



Short communication

## Atomistic insights into role of urea additive in lithium nanoparticles formation

Ruitian He, Kai H. Luo\*

Department of Mechanical Engineering, University College London, Torrington Place, London WC1E 7JE, UK



## ARTICLE INFO

## Keywords:

Urea additive  
 Pyrolysis and oxidation  
 Microexplosion  
 Reactive molecular dynamics  
 Nanoparticles formation  
 Spray flame pyrolysis

## ABSTRACT

Recently, urea additive has been demonstrated to benefit the formation of cathode nanomaterials through spray flame synthesis with improved homogeneity in lithium atoms distribution. Nevertheless, its intrinsic mechanism has not been well understood. In this study, reactive molecular dynamic simulations are performed to gain atomistic insights into the pyrolysis and oxidation mechanisms of a lithium precursor droplet with or without urea additive. A series of comparisons involving the reaction kinetics and pathways of lithium clusters, along with the gas release, energy profiles and morphological characteristics of droplets, is conducted to elucidate the role of urea additive at 1500 K and 0.1 MPa. Urea additive is observed to exert a homogenising impact on the distribution of lithium atoms within the synthesized nanoparticles, as evidenced by the decreased number of large-sized lithium agglomerates and less concentrated lithium element. This can be ascribed to changed reaction pathways of lithium clusters due to urea additive, where the lithium clusters are prone to decompose into fine nanoparticles through initial bonding with urea atoms, followed by bond-breaking to generate gases. The increased amount of gas released from the decomposition of precursor with urea additive leads to a more violent droplet microexplosion, which in turn results in droplet breakup and thus fine droplets. As the ambient temperature is elevated, the presence of urea additive facilitates the formation of fine-sized nanoparticles with enhanced homogeneity of lithium atoms.

### 1. Introduction

Experiments have demonstrated that urea ( $\text{CO}(\text{NH}_2)_2$ ) can serve as a promising agent for producing fine-structured nanomaterials, through both hydrothermal approaches and scalable flame spray pyrolysis (FSP) [1–5]. Specifically, the conventional synthesis process of the widely-used cathode material  $\text{Li}(\text{Ni}_{0.8}\text{Co}_{0.1}\text{Mn}_{0.1})\text{O}_2$  (NCM811), which is generally time-consuming and expensive, can be significantly improved with urea additive via FSP [1,2]. Enhanced homogeneity of lithium atoms within the nanoparticles can be achieved with urea additive via FSP, thereby greatly reducing the calcination time required for the formation of the desired crystal structure and ultimately lowering the manufacturing cost for NCM material [1,2]. To achieve a comprehensive understanding of the role of urea additive in FSP, Deng's group conducted a series of experiments of NCM811 nanomaterials production via urea-assisted FSP, along with one-dimensional macroscopic numerical modelling for a single precursor droplet [1,2]. They visualized the concentration gradients of key elements within the synthesized nanoparticles via FSP as well as the morphological characteristics of a single

precursor droplet. Microexplosion of the precursor droplet is observed to become intensified, triggered by urea additive, which leads to finer final products with uniform element distribution.

Despite extensive recent efforts [1–4], the underlying mechanism for the role of urea additive in the enhanced quality of NCM811 nanomaterials with improved lithium homogeneity [1,2] has not been well understood. Without a fundamental understanding of the role of urea additive in the FSP process, further improvement in the production of nanomaterials via scalable and controllable FSP is difficult to be achieved. Some researchers proposed that the intensified microexplosion is the cause for the improved lithium homogeneity [5–7], but how urea additive influences microexplosion remains unknown. Meanwhile, previous droplet experiments were conducted away from the typical FSP conditions, as common experimental methods face significant challenges under realistic FSP conditions. Furthermore, existing theoretical and/or numerical studies have generally adopted a macroscopic approach with restrictive empirical assumptions, which are unable to gain atomistic insights into the detailed role of urea additive in the FSP process.

\* Corresponding author.

E-mail address: [k.luo@ucl.ac.uk](mailto:k.luo@ucl.ac.uk) (K.H. Luo).<https://doi.org/10.1016/j.cej.2024.154822>

Received 22 April 2024; Received in revised form 29 July 2024; Accepted 12 August 2024

Available online 13 August 2024

1385-8947/© 2024 The Author(s). Published by Elsevier B.V. This is an open access article under the CC BY license (<http://creativecommons.org/licenses/by/4.0/>).

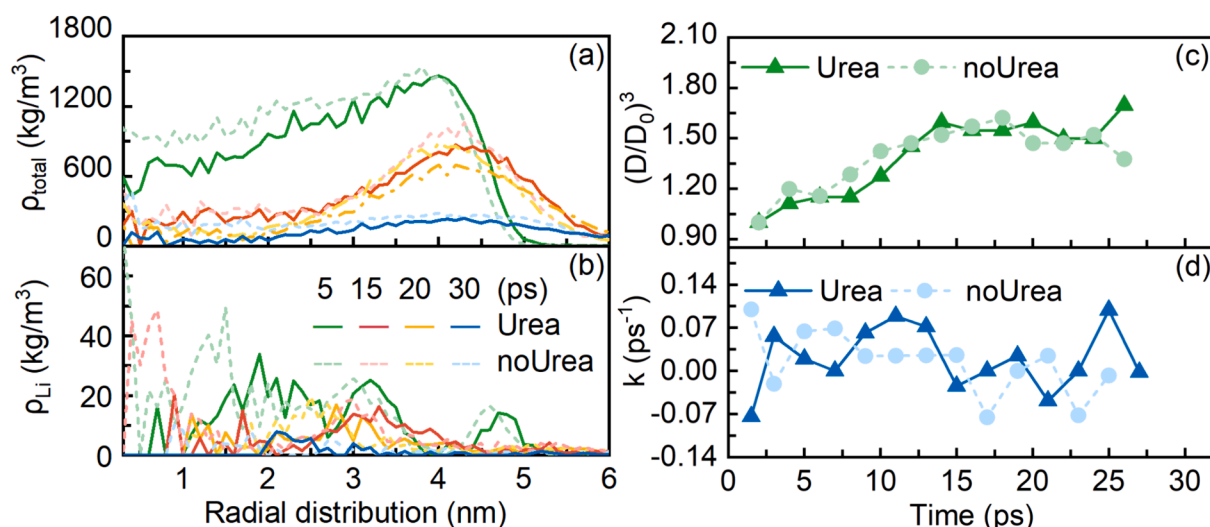


**Fig. 1.** Impact of urea additive on the physical properties of precursor droplets, as indicated by the radial distributions of (a) total density and (b) lithium element density at different time instants, and temporal evolutions of (c) normalized droplet diameter cubed and (d) variation rate of droplet diameter cubed,  $T_a = 1500$  K. The solid and dashed lines denote the results with or without urea additive, respectively.

Therefore, this study aims to shed light on the formation of lithium nanoparticles by performing the reactive molecular dynamic (MD) simulations [8], revealing atomistic mechanisms at play, with a focus on

the role of urea additive. Extensive investigations into reaction kinetics and pathways of lithium clusters formation, along with the decomposed gaseous products, energy profiles and morphological variations of

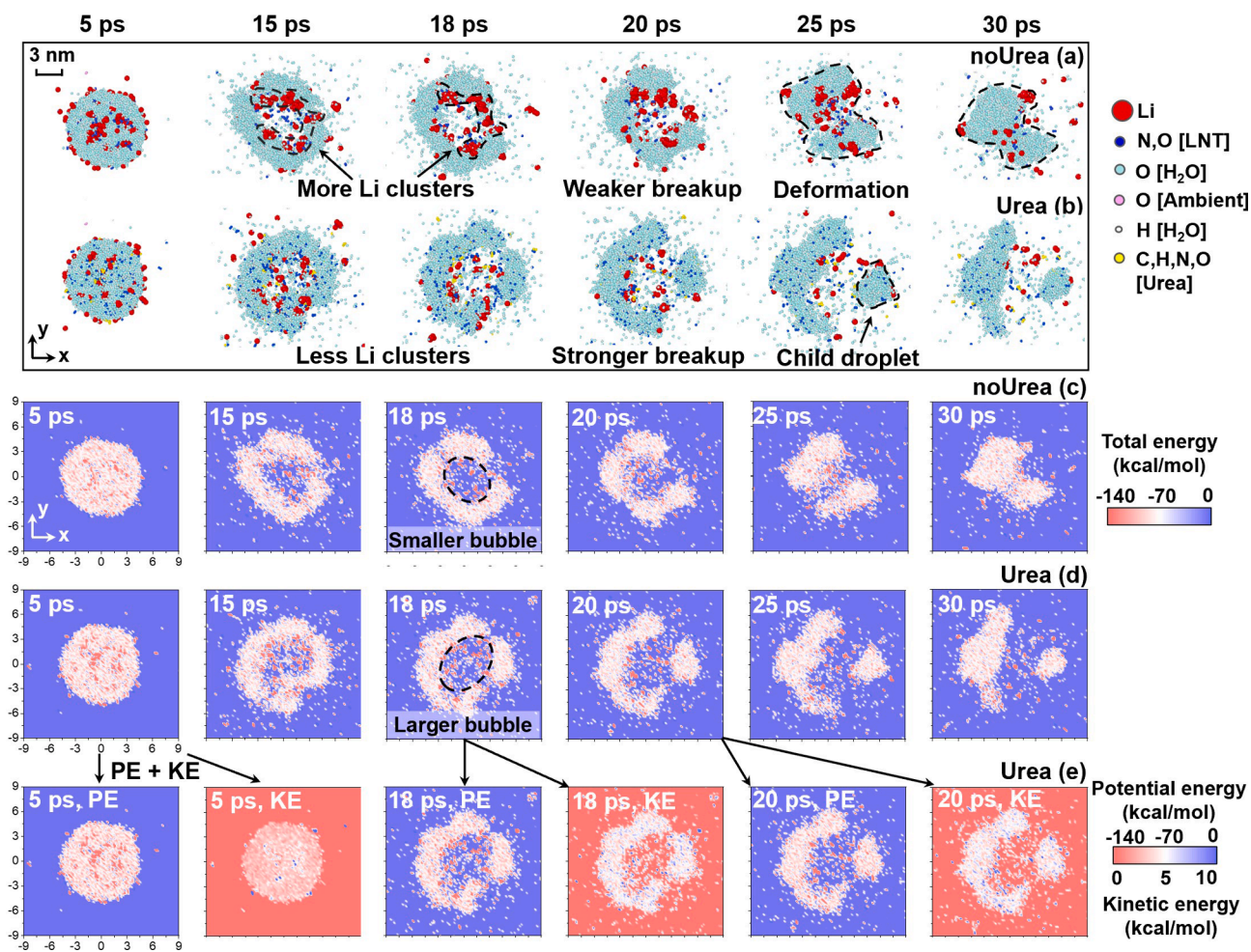


**Fig. 2.** Impact of urea additive on the dynamics of precursor droplets, as indicated by slice views of the droplet (a) without additive and (b) with urea additive, and profiles of total energy (c) without additive and (d) with urea additive, and (e) profiles of potential and kinetic energies with urea additive,  $T_a = 1500$  K. The thickness of slices in the  $z$  direction is 2 nm. 'LNT' denotes lithium nitrate.

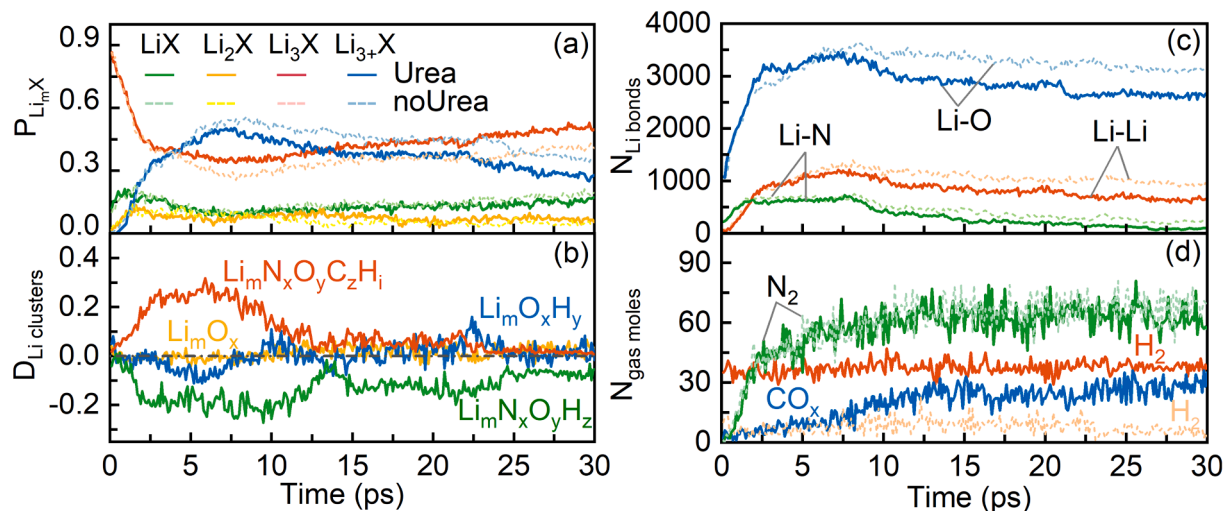


**Fig. 3.** Impact of urea additive on lithium clusters and gaseous products, as indicated by the temporal evolutions of (a) proportions of clusters containing different number of lithium atoms ( $P_{Li_mX}$ ), and (b) differences in proportions of lithium compounds with or without urea ( $D_{Li\_clusters}$ ), and (c) number of lithium bonds ( $N_{Li\_bonds}$ ), and (d) number of gas molecules ( $N_{gas\ moles}$ ),  $T_a = 1500$  K.  $P_{Li_mX}$  and  $D_{Li\_clusters}$  are determined by multiplying the number of  $Li_mX$  by  $n$ , and calculating the difference in the proportions of clusters with or without urea ( $P_{Li_mX,urea} - P_{Li_mX,noUrea}$ ), respectively. The solid lines in darker colours with greater thickness and the dashed lines in lighter colours with thinner thickness in (a), (c) and (d), represent the results with or without urea, respectively.

droplets with or without urea additive are conducted under various ambient temperatures. As a result, the effects of urea additive on gas formation, droplet microexplosion and lithium agglomeration are unravelled.

## 2. Materials and methods

In this study, the bond-order based reactive molecular dynamics method [8] implemented in the LAMMPS package [9] is employed. The force fields for Li/N/O/H/C interactions [10] trained with the quantum mechanics-calculated database are utilized to predict the chemical reactions. A commonly used bond-order cutoff of  $0.3 \text{ \AA}$  is applied to identify the bond connections among various atoms. A spherical precursor droplet with an initial diameter of 10 nm and temperature of 373 K, is constructed in a cubic simulation box with each side length of 40 nm. The ambient, defined as the region from the droplet surface to the lattice boundary, is filled with oxygen gas, and the ambient density is adjusted to maintain the ambient pressure of 0.1 MPa and the ambient temperature range of 1500–3000 K. During the initial heating up period (before 10 ps), the droplet is heated up to a high temperature value, identical to the ambient temperature. The temperature and concentration distributions inside the droplets are set to be homogenous at the start of each simulation. It should be noted that the size of droplets in practical FSP is in the micrometer range, while the adopted droplet size in this study is in the nanometer range due to the excessive computational cost of the ReaxFF MD simulations. It should be emphasized that such a difference in scales would not affect the usefulness of the present study, as the properties of particles produced by practical FSP are determined by key phenomena such as molecular diffusion, chemical reactions and nucleation occurring at the atomic/molecular scales. Therefore, our study aims to provide atomistic insights into the variations in reaction kinetics caused by urea additive and the dynamics of agglomeration of lithium metal atoms within nanoparticles during flame spray pyrolysis. The precursor is composed of lithium nitrate ( $LiNO_3$ ) with a concentration of 2 mol/L dissolved in water. It is noted that this study is not intended to reproduce the NCM811 system studied in the experimental works [1,2]; instead, we focus on unravelling the roles of urea additive and microexplosion in the redistribution of Li atoms in a multi-component Li/N/C/O/H system. To study the effect of urea additive, 2.5 wt% of urea is added, which aligns with the conditions of experiments conducted by Deng et al. [1,2]. The simulation results with

higher urea concentration have been presented in Appendix A. The droplet interface is determined by the commonly utilized '90–10' approach [11], which is calculated based on the densities of the liquid phase and the surrounding. Correspondingly, the equivalent droplet diameter and volume can be identified. Herein, the density is calculated for each radial segment with the same thickness. In each simulation case, a canonical ensemble (NVT) is employed with constant particle/atom number ( $N$ ), constant volume ( $V$ ) and constant temperature ( $T$ ) in the system. The constant temperature is maintained via a Nose-Hoover thermostat by adding dynamic variables coupled to the atom velocities. More details for the simulation configuration can be found in Appendix A as well as our previous work [12].

## 3. Results and discussion

### 3.1. Reaction mechanism of precursor droplets with or without urea additive

In this section, the pyrolysis and oxidization mechanisms of lithium precursor droplets with or without urea additive are investigated under the ambient condition of 1500 K. Figs. 1(a) and 1(b) depict the spatial evolutions of the total and lithium element densities at different time instants, while Figs. 1(c) and 1(d) present the temporal evolutions of normalized droplet diameter cubed and its variation rate, respectively. Figs. 2(a) and 2(b) show the slice views of droplets with or without urea additive, respectively, while Figs. 2(c) and 2(d) present the total energy profiles for these droplets, and Fig. 2(e) displays the potential and kinetic energy profiles of a droplet with urea additive. The text inside the brackets in the chemical symbols in Fig. 2 indicates the source of these atoms. For example, 'O[ambient]' denotes oxygen atoms from the environment. To identify the composition of synthesized lithium compounds, Figs. 3(a) and 3(b) demonstrate the temporal evolutions of proportions of clusters containing different numbers of lithium atoms and differences in lithium clusters with various types of atoms with or without urea, and Figs. 3(c) and 3(d) illustrate the temporal evolutions of lithium bond number and gas molecular number, respectively.

Throughout the entire droplet lifetime, the total density of the precursor droplet gradually diminishes over time, as illustrated in Fig. 1(a). Concurrently, the peak location of the total density gradually shifts away from the droplet core until 15 ns. The droplet diameter keeps increasing before 15 ns, as seen in Fig. 1(c) and Figs. 2(a) and 2(b). This

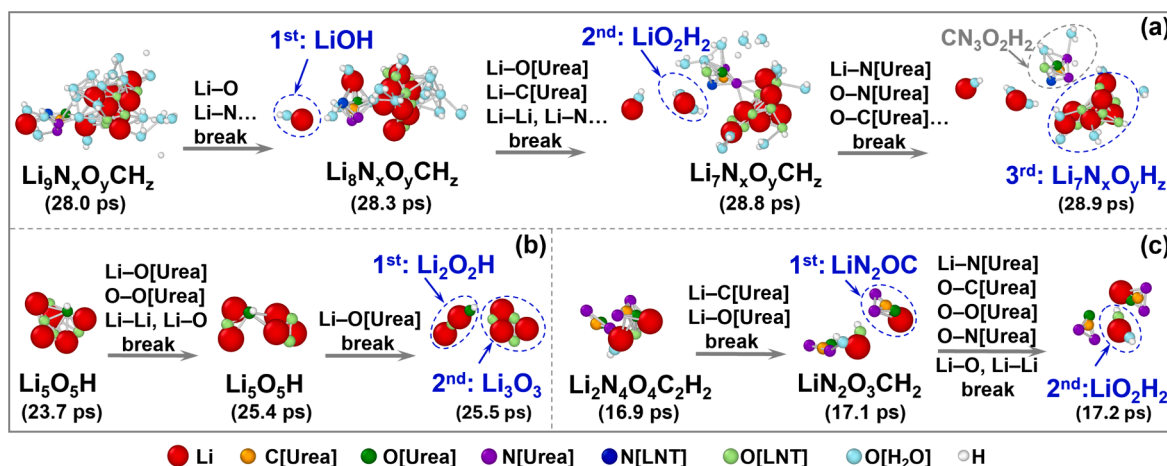


Fig. 4. Reaction pathways of lithium clusters with urea additive (a) clusters containing nine Li atoms, (b) clusters containing five Li atoms and (c) clusters containing two Li atoms,  $T_a = 1500$  K. The primary bond breaking involving lithium and urea atoms is illustrated, and the chemical formulas in blue signify finer lithium products induced by urea additive. (For interpretation of the references to colour in this figure legend, the reader is referred to the web version of this article.)

phenomenon can be attributed to the competition among the precursor consumption, thermal swelling due to increasing temperature, and volume expansion by the growing internal bubble. The energy profiles in Figs. 2(c)–2(e) reflect the dynamics of the precursor droplets. For the droplet with urea additive, it is in the liquid state without any internal bubble at the initial stage (5 ps). The absolute value of potential energy within the droplet exceeds that of kinetic energy by approximately 10 times, as depicted in Fig. 2(e). This leads to a negative value of total energy (the sum of potential and kinetic energies) inside the droplet in Fig. 2(d). The potential energy in the droplet interior gradually increases with time, signifying the production of gases with the less-ordered structure within the droplet.

Despite the seemingly negligible effect of urea additive on the droplet diameter cubed and its variation rate, as shown in Figs. 1(c) and 1(d), the dynamics of the precursor droplets with or without urea exhibit significant disparities. Specifically, the presence of urea facilitates the consumption of the precursor (tending to reduce the droplet size), as indicated by the lower total density of droplet in Fig. 1(a). Conversely, more gases are released during the decomposition of precursor with urea additive in Fig. 3(d), which would lead to volume expansion of droplet due to the enlarged internal bubble, as indicated by the expanded region with the increased total energy inside the droplet at 18 ps in Figs. 2(c) and 2(d). The detailed effect of released gas on the droplet and simulation system can be found in Appendix A. Consequently, the combined effects of precursor consumption and gas production contribute to a small overall difference in droplet size in the cases with or without urea. More importantly, urea additive gives rise to the more uniformly distributed lithium atoms within the droplet, as observed from the density profile of lithium element in Fig. 1(b). The decreased number of large-sized lithium agglomerates ( $\text{Li}_{3+X}$ ) also implies the improved homogeneity of lithium atoms inside the droplet, as evidenced by the cluster profile in Fig. 3(a) and snapshots in Figs. 2(a) and 2(b). These results indicate that urea additive facilitates the formation of fine-structured metal oxide nanoparticles at the atomistic scale, in qualitative agreement with experimental results [1,2].

It was proposed that droplet microexplosion became more intensified due to urea additive, ultimately contributing to the enhanced uniformity of lithium atoms within final nanoparticles [1]. Here we analyse the underlying mechanism of role of urea additive in the reaction pathways from the precursor clusters to fine lithium products. Firstly, the intensity of droplet microexplosion is indeed observed to be elevated with urea additive. In the case without urea, a gas bubble appears in the centre of the droplet, which bursts by 20 ps in Fig. 2(a). However, the droplet as a whole has not broken up; instead, it retracts to form a

deformed droplet by 25 ps. Throughout this process, the lithium atoms are concentrated in certain areas. In contrast, droplet microexplosion becomes more intensified with urea additive. The strengthened microexplosion causes a rapid disintegration of the entire droplet, followed by the formation of a child droplet at 20 ps in Fig. 2(b). The elevated intensity of microexplosion mainly stems from the increased quantity of gaseous products released and trapped in the droplet interior. As depicted in Fig. 3(d), more hydrogen gas and carbon oxides are produced with urea additive, which results in an enlarged internal bubble at 18 ps, as compared in Figs. 2(c) and 2(d).

At the fundamental level, the influence of urea additive on the formation of fine lithium products can be explained by the variations in the reaction pathways of precursor clusters. Three typical reaction pathways of lithium clusters comprising different numbers of lithium atoms with urea additive are illustrated in Fig. 4. With urea additive, the bond connections among different lithium atoms become weak, as evidenced by the reduced number of Li–Li bonds in Fig. 3(c). Instead, they tend to bond with atoms in urea molecules to form lithium compounds with the chemical formula of  $\text{Li}_m\text{N}_x\text{O}_y\text{C}_z\text{H}_i$ , as inferred by the positive differences in the proportions of  $\text{Li}_m\text{N}_x\text{O}_y\text{C}_z\text{H}_i$  in Fig. 3(b). Taking  $\text{Li}_9\text{N}_x\text{O}_y\text{CH}_z$  in Fig. 4(a) as an example, it is generated via bonding among lithium, oxygen, carbon and nitrate atoms from urea molecules. However, the numbers of Li–O and Li–N bonds are not increased as expected, as seen in Fig. 3(c). This is because the bonds connecting lithium, oxygen, carbon and nitrate atoms from urea molecules rapidly break down, as depicted in Fig. 4, decomposing the large lithium cluster and finally yielding several small lithium oxides products, i.e., LiOH and  $\text{Li}_2\text{O}_2\text{H}$ . Similarly, lithium clusters comprising five and two lithium atoms in Figs. 4(b) and 4(c), respectively, decompose into fine lithium nanoparticles, such as  $\text{Li}_3\text{O}_3$  and  $\text{Li}_2\text{O}_2\text{H}$ . The differences in lithium bond number with or without urea additive become noticeable from 8 ns onwards (Fig. 3(c)), and the variations in the probabilities of large lithium clusters ( $\text{Li}_3\text{X}$  and  $\text{Li}_{3+X}$ ) start from the same time instant (Fig. 3(a)), which also demonstrates the role of urea additive in forming fine lithium clusters by altering their bond connections. Throughout this process, several by-products of urea, such as ammeline and ammeline ( $\text{C}_7\text{N}_x\text{O}_y\text{H}_z$ ) are captured, as indicated by the grey dashed circle in Fig. 4(a), which is aligned with thermogravimetric experimental results of urea [13–15]. In general, urea additive prevents the accumulation of lithium atoms into clusters by altering the reaction pathways of lithium-related reactions.

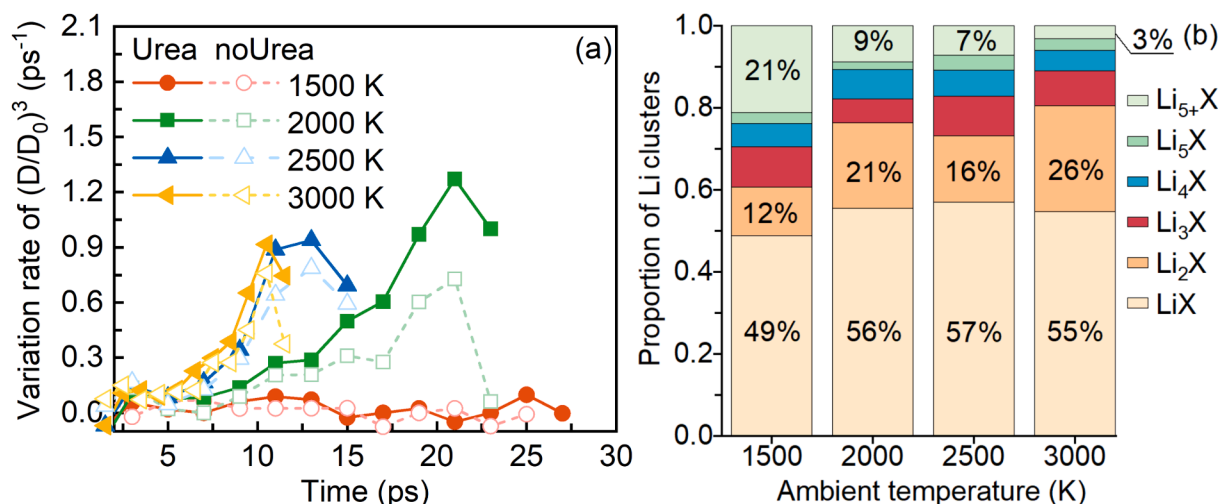


**Fig. 5.** Impact of ambient temperature on the droplet characteristics and synthesized lithium clusters (a) temporal evolution of variation rate of normalized diameter cubed of the droplet with or without urea additive (b) proportion of clusters containing various numbers of lithium atoms, at the time when the droplet with urea additive explodes,  $T_a = 1500\text{--}3000$  K. The curves of variation rate of droplet size cease at the time of droplet fragmentation. The proportion of  $\text{Li}_m\text{X}$  is calculated by  $m \cdot N_{\text{Li}_m\text{X}}/N_{\text{Li}}$ , where  $N_{\text{Li}_m\text{X}}$  and  $N_{\text{Li}}$  are the number of  $\text{Li}_m\text{X}$  and total number of lithium atoms in the system, respectively.

### 3.2. Impact of urea additive at various ambient temperatures

Unlike the nearly constant variation rate of droplet diameter cubed at 1500 K in Section 3.1, the precursor droplets with or without urea additive feature distinct behaviours at higher ambient temperatures ranging from 2000 to 3000 K, as displayed in Fig. 5(a). Taking the case with urea at 2000 K as an example, the variation rate of droplet diameter cubed initially increases to a peak value of  $1.27 \text{ ps}^{-1}$  at 21 ps and then promptly decreases. However, as the ambient temperature is further elevated, the influence of urea additive on the droplet characteristics gradually diminishes, reflected by the reducing difference in droplet diameter cubed. To quantify the composition of synthesized lithium nanoparticles, Fig. 5(b) shows the proportion of synthesized clusters containing various numbers of lithium atoms at the time when the droplet fragments. As the ambient temperature rises from 1500 to 2000 and 3000 K, the proportion of agglomerates containing more than five lithium atoms ( $\text{Li}_{5+}\text{X}$ ) rapidly decreases from 21%, 9% to 3%. Meanwhile, the proportions of  $\text{LiX}$  and  $\text{Li}_2\text{X}$  progressively climb from 49%, 56% to 55% and 12%, 21% to 26%, respectively. These observations suggest that urea additive enhances the production of fine lithium nanoparticles with increasing ambient temperature.

## 4. Conclusions

This work has elucidated the role of urea additive in nanoparticle synthesis by conducting reactive MD simulations of lithium precursor nanodroplets exposed to various ambient temperatures. Comprehensive analyses of reaction kinetics and pathways of lithium clusters, along with the gas products, energy profiles and morphological characteristics of droplets are carried out. The presence of urea additive facilitates the uniform distribution of lithium atoms within the synthesized nanoparticles, as indicated by the less concentrated density profile of lithium atoms and the decreased amount of large lithium agglomerates. The underlying cause for the formation of fine lithium nanoparticles lies in the changed reaction pathways of precursor clusters due to urea additive. Specifically, large lithium clusters decompose into several small oxide nanoparticles through initial bonding with urea atoms and then bond-breaking. Additionally, the changed reaction pathways caused by urea additive trigger more intensified droplet microexplosion into smaller droplets, evidenced by the enlarged internal bubble stemming from the increased amount of decomposed gases trapped in the droplet interior, such as carbon oxides and hydrogen gases. As the ambient

temperature rises from 1500 to 3000 K, the effect of urea additive on the improved homogeneity of lithium atoms within the nanoparticles first picks up and then moderates.

### CRediT authorship contribution statement

**Ruitian He:** Writing – original draft, Visualization, Validation, Software, Methodology, Investigation, Formal analysis, Conceptualization. **Kai H. Luo:** Conceptualization, Formal analysis, Project administration, Funding acquisition, Supervision, Writing – review & editing.

### Declaration of competing interest

The authors declare that they have no known competing financial interests or personal relationships that could have appeared to influence the work reported in this paper.

### Data availability

Data will be made available on request.

### Acknowledgements

The work is supported by the UK Engineering and Physical Sciences Research Council (EPSRC) under Grant No. EP/T015233/1. ARCHER2 supercomputing resources provided by the EPSRC under the project ‘‘UK Consortium on Mesoscale Engineering Sciences (UKCOMES)’’ (Grant No. EP/X035875/1) are also acknowledged. This work made use of computational support by CoSeC, the Computational Science Centre for Research Communities, through UKCOMES.

### Appendix A. Supplementary data

Supplementary data to this article can be found online at <https://doi.org/10.1016/j.cej.2024.154822>.

### References

- [1] M. Bhat, S. Luo, J. Zhang, C. Zhang, B. Zhou, S. Deng, Multi-component precursor droplet evaporation in spray synthesis of cathode materials, *Chem. Eng. J.* 479 (2024) 147417.

- [2] J. Zhang, V.L. Muldoon, S. Deng, Accelerated synthesis of  $\text{Li}(\text{Ni}_{0.8}\text{Co}_{0.1}\text{Mn}_{0.1})\text{O}_2$  cathode materials using flame-assisted spray pyrolysis and additives, *J. Power Sources* 528 (2022) 231244.
- [3] L.J. Vasquez-Elizondo, J.C. Rendón-Ángeles, Z. Matamoros-Veloz, J. López-Cuevas, K. Yanagisawa, Urea decomposition enhancing the hydrothermal synthesis of lithium iron phosphate powders: effect of the lithium precursor, *Adv. Powder Technol.* 28 (2017) 1593–1602.
- [4] H. Du, K. Huang, M. Li, Y. Xia, Y. Sun, M. Yu, B. Geng, Gas template-assisted spray pyrolysis: A facile strategy to produce porous hollow  $\text{Co}_3\text{O}_4$  with tunable porosity for high-performance lithium-ion battery anode materials, *Nano Res.* 11 (3) (2018) 1490–1499.
- [5] C.D. Rosebrock, T. Wriedt, L. Mädler, K. Wegner, The role of microexplosion in flame spray synthesis for homogeneous nanopowders from low-cost metal precursors, *AIChE J.* 62 (2) (2016) 381–391.
- [6] J. Shinjo, J. Xia, L.C. Ganippa, A. Megaritis, Physics of puffing and microexplosion of emulsion fuel droplets, *Phys. Fluids* 26 (2014) 103302.
- [7] F. Meierhofer, H. Li, M. Gockeln, R. Kun, T. Grieb, A. Rosenauer, U. Fritsching, J. Kiefer, J. Birkenstock, L. Mädler, S. Pokhrel, Screening precursor–solvent combinations for  $\text{LiTi}_5\text{O}_{12}$  energy storage material using flame spray pyrolysis, *ACS Appl. Mater. Interfaces* 9 (43) (2017) 37760–37777.
- [8] A.C.T. van Duin, S. Dasgupta, F. Lorant, W.A. Goddard, ReaxFF: a reactive force field for hydrocarbons, *J. Phys. Chem. A* 105 (2001) 9396–9409.
- [9] S. Plimpton, Fast parallel algorithms for short-range molecular dynamics, *J. Comput. Phys.* 117 (1) (1995) 1–19.
- [10] M.Y. Yang, S.V. Zybin, T. Das, B.V. Merinov, W.A. Goddard, E.K. Mok, H.J. Hah, H. E. Han, Y.C. Choi, S.H. Kim, Characterization of the solid electrolyte interphase at the Li metal–ionic liquid interface, *Adv. Energy Mater.* 13 (3) (2023) 2202949.
- [11] J. Lekner, J.R. Henderson, Surface tension and energy of a classical liquid–vapour interface, *Mol. Phys.* 34 (2) (1977) 333–359.
- [12] D. Hou, G. Wang, J. Gao, K.H. Luo, Molecular dynamics study on evaporation of metal nitrate-containing nanodroplets in flame spray pyrolysis, *Nanoscale* 15 (2023) 5877–5890.
- [13] C. Xia, Y. Zhu, D. Liu, S. Zhou, Y. Feng, J. Shi, Y. Jun, Newly developed detailed urea decomposition mechanism by marine engine urea-SCR system crystallization test and DFT calculations, *Chem. Eng. J.* 470 (2023) 144176.
- [14] S. Tischer, M. Börnhorst, J. Amsler, G. Schochb, O. Deutschmann, Thermodynamics and reaction mechanism of urea decomposition, *Phys. Chem. Chem. Phys.* 21 (2019) 16785.
- [15] P.M. Schaber, J. Colson, S. Higgins, D. Thielen, B. Anspach, J. Brauer, Thermal decomposition (pyrolysis) of urea in an open reaction vessel, *Thermochim. Acta* 424 (1–2) (2004) 131–142.